ID and 2D Electron Spin Resonance Imaging (ESRI) of Nitroxide Radicals in Stabilized Poly(acrylonitrile−butadiene−styrene) (ABS): UV vs Thermal Degradation

Krzysztof Kruczala,[†] Mikhail V. Motyakin, and Shulamith Schlick*

Department of Chemistry, University of Detroit Mercy, Detroit, Michigan 48219-0900

Received: December 2, 1999; In Final Form: January 27, 2000

We present the application of 1D spatial and 2D spatial-spectral electron spin resonance imaging (ESRI) in order to deduce the intensity profile and the spatial variation of line shapes for nitroxides formed during accelerated UV irradiation and thermal degradation of poly(acrylonitrile−butadiene−styrene) (ABS) containing a hindered amine stabilizer (HAS). The detection of two dynamically different sites for the HAS-derived nitroxide radicals ("fast" and "slow" components) and the decrease of the relative intensity of the fast component with UV irradiation or heating time point to the butadiene-rich domains as the vulnerable site for degradation. Spatial variation of the nitroxide intensity *and* of the line shapes was detected in the UV-irradiated samples. The nitroxide signal is strong on the irradiated side, increases with time on the opposite side, and is very weak in the sample interior; these results were taken as evidence for diffusion-limited oxidation. By contrast, the radical concentration *and* the line shapes are spatially homogeneous in the polymer undergoing thermal degradation at 333 K. This study has demonstrated the potential of imaging methods based on ESR to provide details on polymer degradation and stabilization that cannot be deduced from properties averaged over the entire sample.

Introduction

Degradation of polymeric materials upon exposure to heat, mechanical stress, and ionizing or UV irradiation in the presence of oxygen is the polymer equivalent to metal corrosion.[1−6] The degradation process is accelerated by chromophores, free radicals, and metallic residues from the polymerization reactions. Often the deleterious effects are not immediately detected, but develop over longer periods. While the time scale of these changes may vary, the final results are degradation of the structure and collapse of the mechanical properties. The accelerated rate of ozone depletion in the stratosphere due to environmental factors is expected to raise the level of UV-B radiation (≈290−320 nm)[7] and to increase the severity of problems associated with polymer deterioration.

Hindered amine stabilizers (HAS) rank among the most important additives used for light and heat stabilization of polymers. Nitroxides and hydroxylamine ethers are the major products of reactions involving HAS. The HAS-derived nitroxides are relatively stable, but react with free radicals (as "scavengers") to yield diamagnetic species; the hydroxylamine ethers can regenerate the original nitroxide, thus resulting in an efficient protective effect.[3,5] So far the complex protective mechanism offered by HAS is known only in broad terms.[3−6]

We have initiated a study of HAS behavior in poly(acrylonitrile−butadiene−styrene) (ABS) exposed to UV radiation, using electron spin resonance imaging (ESRI). Imaging is based on encoding spatial information in the ESR spectra via magnetic field gradients.[8,9] In the first communication on this subject we have presented concentration profiles, obtained by 1D ESRI, of HAS-derived nitroxides as a function of UV irradiation time of the polymer in a weathering chamber.[10] The ESR spectra consist of a superposition of two components differing in their dynamical properties, slow ("S") and fast ("F"). The imaging experiments mapped the intensity of the HAS-derived nitroxide radicals along the irradiation direction, and suggested a spatial variation of the corresponding ESR line shapes. This report[10] demonstrates the potential of ESRI to providing details on degradation and stabilization that are crucial for elucidating the degradation mechanism.

The spatial variation of line shapes is not only of academic interest: as the F component can be identified with nitroxides in low-T_g butadiene-rich domains (T_g is the glass transition temperature), the ability to detect and determine the relative intensities of the two spectral components as a function of irradiation depth is important for identifying where and how the chemistry takes place. The present paper describes the application of 2D spatial-spectral ESRI in order to follow *nondestructively* the spatial variation of the line widths and of the relative intensity of both spectral components along the sample depth. In addition, we demonstrate by 1D and 2D ESRI the contrasting degradation results in UV irradiation compared to thermal degradation.

2D spatial-spectral ESRI images from "phantom" samples consisting of two types of spectra have been reported previously.[11] To the best of our knowledge this paper presents, for the first time, the application of this method to the detection and quantitative analysis of the spatial variation of the ESR line shapes in a real system.[12]

Experimental Section

Sample Preparation. Accelerated degradation experiments were performed by exposure to UV irradiation of poly(acrylonitrile−butadiene−styrene) (ABS Magnum 342 EZ, from Dow Chemical Company) doped with 2% w/w of (bis(2,2,6,6-

* Author to whom correspondence should be addressed. E-mail: schlicks@udmercy.edu.

[†] On leave from the Faculty of Chemistry, Jagiellonian University, Ingardena 3, 30-060 Cracow, Poland.

10.1021/jp994247y CCC: $19.00
Published on Web 03/24/2000

CHART 1

(a) Repeat Units in ABS Polymers

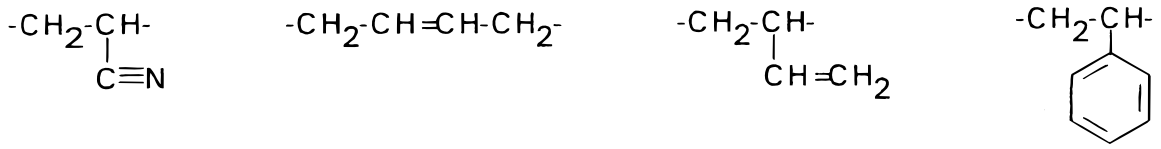

(b) Hindered Amine Stabilizer (HAS): Tinuvin 770

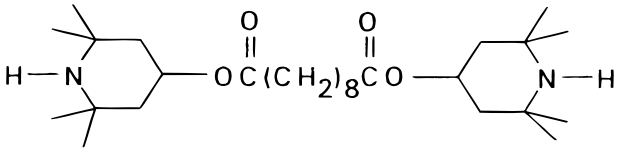

tetramethyl-4-piperidinyl) sebacate), the HAS known as Tinuvin 770 from Ciba Specialty Chemicals Corporation (Chart 1). The polymer and the HAS were blended, shredded, and shaped into 10 cm × 10 cm × 0.4 cm plaques in an injection molding machine at 483 K. The plaques were exposed on one side to UV radiation in a Ci35 Weather-ometer located at the Ford Research Laboratories. The irradiation chamber allows simultaneous control of the temperature (black panel temperature 338 K) and humidity (dew point 298 K). The irradiation intensity was 0.45 W/m^2, comparable with the average summer noontime solar intensity in Miami, FL. The plaques were irradiated continuously. For the ESR imaging experiments, cylindrical samples 4 mm in diameter were cut from the plaques, with the cylinder axis along the direction of the UV radiation. The samples were placed in the ESR resonator with the symmetry axis along the field gradient. Thermal degradation at 333 K was performed on the same samples. Additional details have been reported.[10]

The results reported here are based on the study of eight plaques, of which six contained HAS and two were control samples (without HAS). Of the six plaques containing HAS two had their back side (non exposed to UV) covered with Al foil. No ESR signals were detected before or after UV irradiation in the control plaques. In the plaques that contained HAS, a very weak nitroxide signal was detected before irradiation or thermal treatment; this signal was negligible compared to the signal detected after the shortest UV irradiation time (23 h). Only minor variations in the nitroxide intensity were detected between samples taken from different plaques.

ESR Imaging. The ESR imaging system in our laboratory consists of the Bruker 200D ESR spectrometer with an EMX console, and equipped with two Lewis coils and two regulated DC power supplies. The coils supply a maximum linear field gradient of ≈320 G/cm in the direction parallel to the external magnetic field, or ≈250 G/cm in the vertical direction (along the long axis of the microwave resonator), with a control current of 20 A applied to each coil.[8−10]

In 1D ESRI experiments the concentration profile is deduced from two spectra, one in the presence and one in the absence of the field gradient.[9,10,13] In the presence of a gradient, the ESR spectrum is a convolution of the spectrum in the absence of the gradient with the distribution of the paramagnetic centers along the gradient direction. The convolution is correct only if the ESR line shape *has no spatial dependence*. The concentration

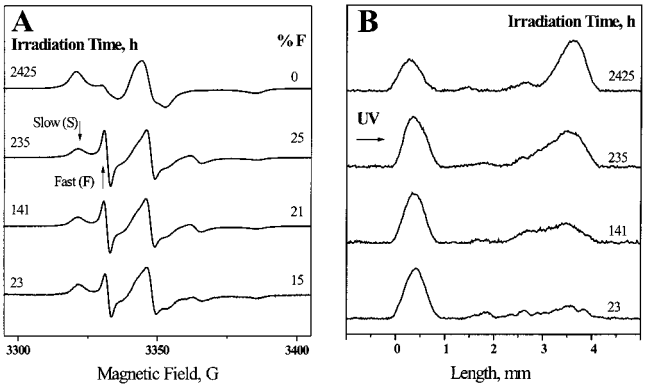

Figure 1. (A) X-band ESR spectra at 300 K of an ABS polymer containing HAS for the indicated UV-irradiation times. Upward and downward arrows point, respectively, to signals from the "fast" and "slow" spectral components. The percentage of the "fast" component, %F, in each case is indicated. (B) Concentration profiles of HAS-derived nitroxides for the indicated UV irradiation times in the weathering chamber. The horizontal arrow indicates the irradiated side of the sample.

profiles were obtained by deconvolution of the line shape measured in the presence of gradients.[10,11,13] No correction for the sensitivity profile of the ESR cavity is needed if the sample is <4 mm long.

Each 2D spatial spectral image was reconstructed from a complete set of projections collected as a function of the magnetic field gradient, using a convoluted back-projection algorithm.[8,14] The number of points for each projection (1024) was kept constant. The maximum experimentally accessible projection angle α_{max} is determined by the maximum gradient G_{max}: $\tan\alpha_{max} = (L/\Delta H)\, G_{max}$, where L is the spatial dimension, and ΔH is the spectral width. The maximum sweep width is $SW_{max} = \sqrt{2}\Delta H/\cos\alpha_{max}$. For a width $\Delta H \approx 65$ *G*, which was dictated by the slow-motional spectral component (S), a sample length of 0.4 cm and a maximum field gradient of 250 *G*/cm, $\alpha_{max} = 57°$ and $SW_{max} = 169$ *G*. A complete set of data consisted of 64 projections, taken for gradients corresponding to equally spaced increments of α in the range $-90°$ to $+90°$; of these projections, typically 41 were experimentally accessible and the rest were projections at missing angles. The projections at the missing angles were assumed to be the same as those measured at α_{max}. Each projection required 1−3 scans, and each scan was obtained with scan time 41 s, microwave power 2−6

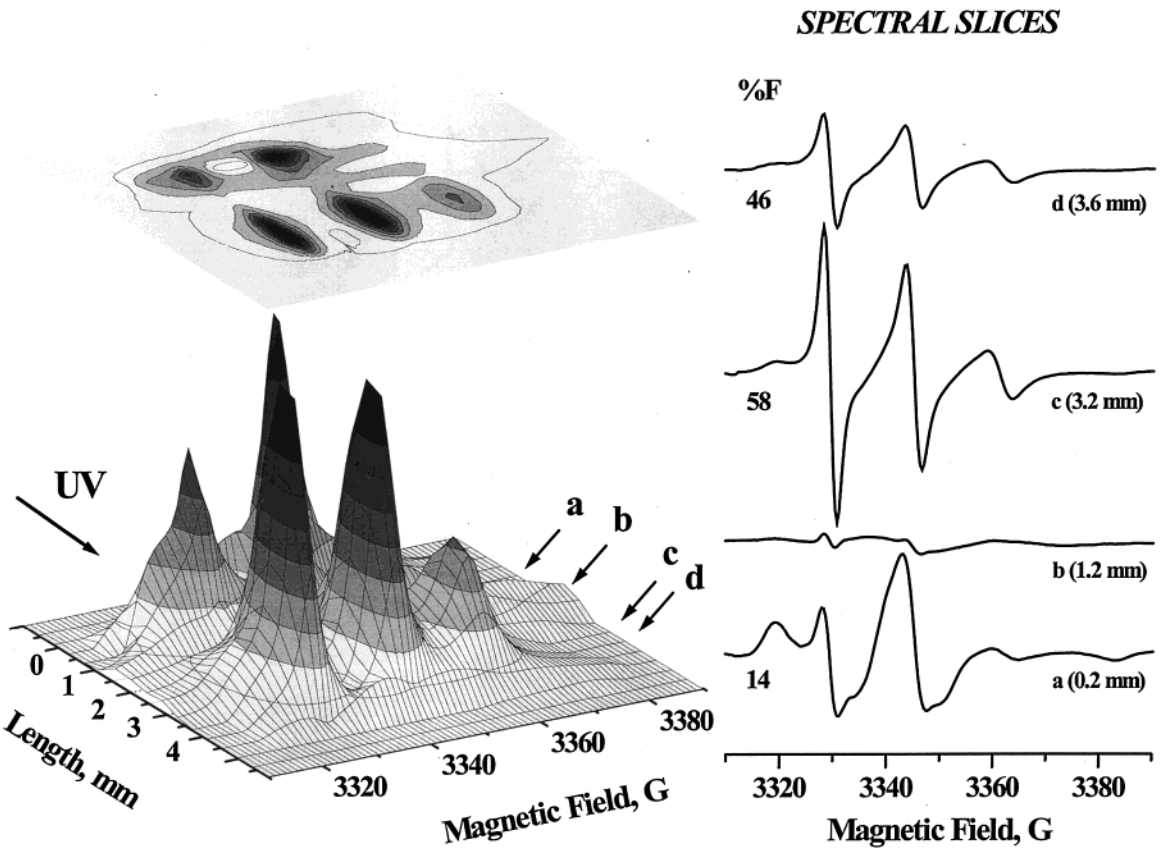

Figure 2. 2D spatial-spectral contour (top) and perspective (bottom) plots of HAS-derived nitroxides after 141 h UV irradiation in the weathering chamber, presented in absorption. The spectral slices a, b, c, and d for the indicated depths are presented in the derivative mode; these slices were obtained by averaging signals from sample sections within ±0.20 mm of the position indicated by the arrow in the perspective plot. %F is shown for the a, c, and d slices.

mW, modulation 1 or 2 *G*, time constant of 41−82 ms and gain $1-2 \times 10^4$. The reconstruction algorithm produced the image on a 256 × 256 grid. For display, the number of points for each coordinate can be chosen (64, 128, or 256 points); in most cases the 2D images were displayed with 16 points for the spatial coordinate and 256 for the spectral coordinate.

Results and Discussion

X-band ESR spectra at 300 K of the HAS-derived nitroxide in UV-irradiated ABS, for the indicated irradiation time in the weathering chamber, are presented in Figure 1A. All spectra, except that corresponding to the longest irradiation time, consist of a superposition of two components, from nitroxide radicals differing in their mobility: a "fast" component (F) with a total width of 32.2 G, and a "slow" component (S) with a spectral width of 64.2 G. The spectra indicate the presence of HAS-derived nitroxide radicals in two different environments. It is reasonable to assume that the fast and slow components reflect nitroxides located, respectively, in low-T_g domains dominated by polybutadiene sequences ($T_g \approx 200$ K), and in high-T_g domains dominated by polystyrene ($T_g \approx 370$ K) or polyacrylonitrile sequences ($T_g \approx 360$ K). The relative intensity of the "fast" component decreases with increasing irradiation time, and is negligible for $t = 2425$ h. By subtracting the spectrum of the slow component (in the upper spectrum) from the composite spectrum and superimposing the two components, it was possible to reproduce the composite spectra shown in Figure 1A and, by double integration, to determine the relative concentration of each component. The percentage of the fast component calculated in this way, %F, is given in Figure 1A. The relative intensity of the F component as a function of irradiation time increases to a maximum, decreases, and becomes negligible at the longest irradiation time. We propose that the decrease of the relative intensity of F with irradiation time is due to the consumption of the HAS-derived nitroxide radicals located in the butadiene-rich domains of the polymer, as butadiene is expected to be more vulnerable to degradation[15] compared to the other repeat units in ABS. The ESR spectra establish therefore the connection between the nitroxide concentration and its line shape, and the degradation process.

Because the convolution procedure is valid only for spatially invariant line shapes, we measured the 1D images at 240 K; at this temperature both spectral components are in the slow-motional regime and have the same line shape. In Figure lB we present the concentration profile along the irradiation depth, deduced by deconvolution of images measured at 240 K. The spectral resolution is ≈0.3 mm (based on the broader signals at 240 K). The larger nitroxide concentration near the outer planes of the sample and the gradual increase of the nitroxide concentration at the non-irradiated side clearly indicate the combined effects of oxygen and UV radiation, and show the regions where the chemistry takes place: If oxygen diffusion is slow compared to the rate of degradation, only surfaces in contact with air are degraded, while the sample interior is little, if at all, affected; this is the diffusion-limited oxidation (DLO).[16] We note that the same conclusions are valid for samples whose back was covered with aluminum foil, indicating that the radicals present on the back side are not due to direct irradiation, for instance by scattered light.

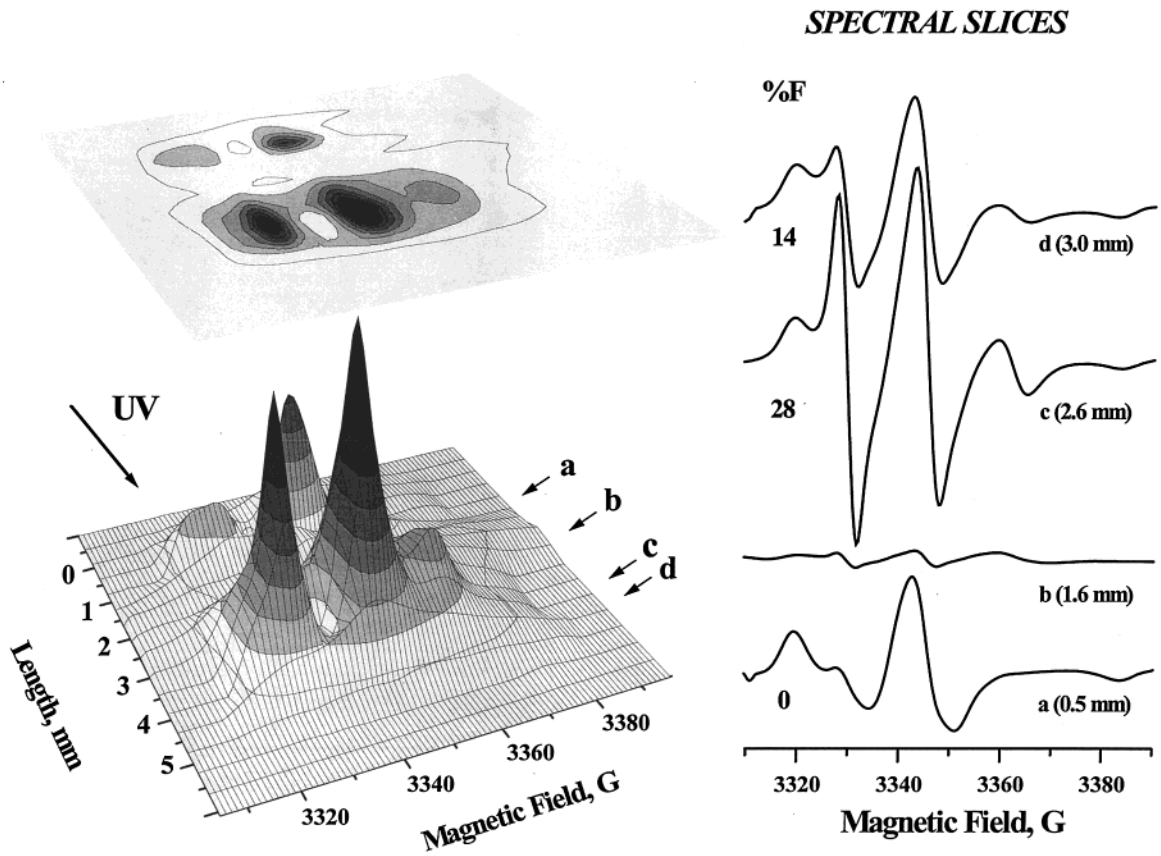

Figure 3. 2D spatial-spectral contour (top) and perspective (bottom) plots of HAS-derived nitroxides after 934 h of UV irradiation in the weathering chamber, presented in absorption. The spectral slices a, b, c, and d for the indicated depth are presented in the derivative mode; these slices were obtained by averaging the signals from sample sections within ±0.20 mm of the position indicated by the arrow in the perspective plot. %F is shown for the a, c, and d slices.

In order to shed light on the spatial variation of the two spectral components, we performed 2D ESRI on the UV-irradiated polymer, and compared the results with those of the thermally degraded ABS polymer. In Figures 2 and 3 we present 2D spatial-spectral perspective and contour images of nitroxide radicals in ABS UV-irradiated for 141 and 934 h, respectively, in the weathering chamber. The ESR intensity is presented in absorption mode. To the right of Figures 2 and 3 we also present spectral slices (in the derivative mode) at the indicated depth of the sample; these slices were obtained by averaging signals from slices within ±0.20 mm. The contour plots in Figures 2 and 3 show very clearly the distribution of the signal intensity, and the negligible signal intensity in the sample interior, as also seen in the concentration profiles (Figure 1B) deduced from 1D ESRI. The spectral slices indicate not only the line shape variation but also the relative intensity of each spectral component as a function of depth. For the short irradiation time ($t = 141$ h) the ESR spectrum of the directly irradiated part of the sample exhibits a composite spectrum with %F ≈ 14%; at and near the non-irradiated side %F is significantly larger. After 934 h of irradiation, the irradiated side contains no fast component, and %F is significantly lower at and near the non-irradiated side. We note that section "**b**" in Figure 3 represents a very weak signal and %F was not calculated for this section.

The major conclusion from the 2D images presented in Figures 2 and 3 is that the nitroxides in the butadiene-rich domains is consumed rapidly on the irradiated side, and decreases to zero after 934 h of irradiation. On the non-irradiated side the degradation is much slower, but even on this side a decrease of %F is detected when the irradiation time increases from 141 h to 934 h.

In Figure 4 we present the 2D spatial-spectral perspective and contour images, and the spectral slices of nitroxides in ABS thermally degraded during 796 h. These samples were kept at 333 K in a constant temperature bath. In contrast to the UV-irradiated samples, the nitroxide distribution is essentially homogeneous along the sample depth, as also seen in 1D profiles (not presented); moreover, no spatial variation of the line shapes was detected, and on the average %F = 27 ± 4%. This F content deduced by 2D ESRI is in agreement with results of sectioning the sample, and weighing and determining the %F in each slice; the average F content in the cut sample was 26 ± 4%.

Some of the features of thermal degradation are visually more clear in the first derivative mode presentation of the 2D images, Figure 5, where the F and S components are indicated by arrows. The intensity of the nitroxide signal is significantly lower in the thermally degraded polymer compared to the UV-irradiated samples, by a factor of ≈5−15. It seems that the rate of oxygen transport is in this case comparable with the rate of thermal degradation, and the process in not diffusion-limited as in the case of the UV-irradiation.

In conclusion, we presented 1D and 2D spatial-spectral ESR images that indicate the spatial variation of the nitroxide intensity and of the line shapes for HAS-derived nitroxides in ABS. The spatial evolution of the relative intensity of each spectral component was calculated from these images. The information obtained reflects the degradation mechanism and the difference between UV- and thermal degradation of the ABS polymer.

Methods for measuring the spatial distribution of polymer properties due to degradation have been developed by other groups: Density profiling measures the change in density, which is expected to increase in aged samples, along the irradiation

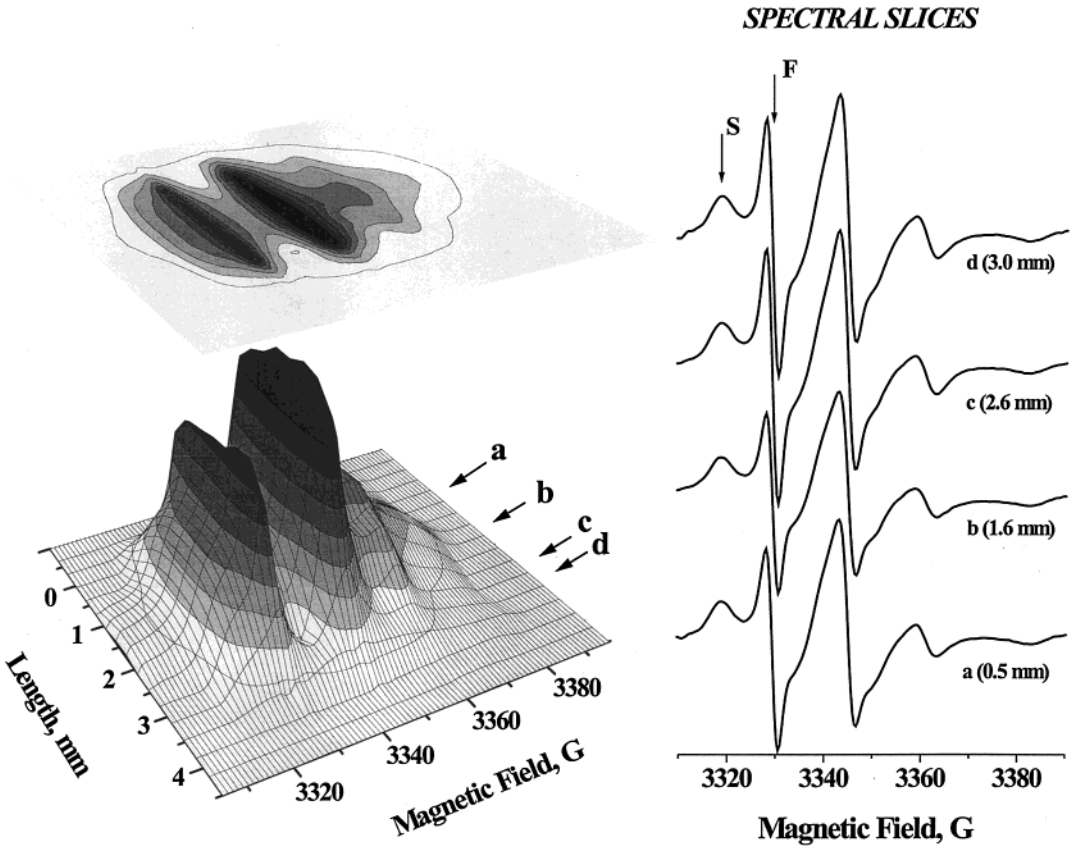

Figure 4. 2D spatial-spectral contour (top) and perspective (bottom) plots of HAS-derived nitroxides in ABS after 796 h thermal degradation at 333 K, presented in absorption. The spectral slices a, b, c, and d for the indicated depths are presented in the derivative mode; these slices were obtained by averaging the signals from sample sections within ±0.20 mm of the indicated position. The average %F is 27 ± 4 (see text).

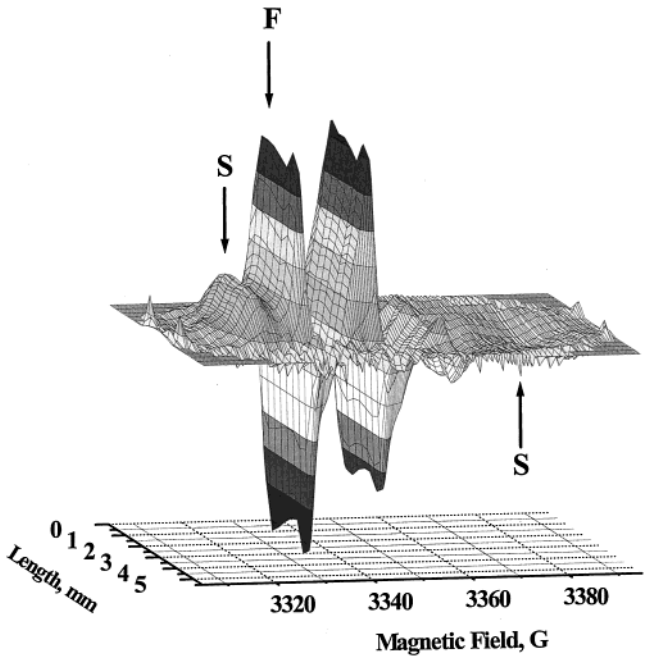

Figure 5. 2D spatial-spectral perspective plot of HAS-derived nitroxides after 796 h thermal degradation at 333 K, presented in the first derivative. Note the homogeneous distribution of the radicals. Signals for the S and F components are indicated by arrows.

depth;[17] and modulus profiling measures the tensile modulus, which decreases during degradation.[18,19] The spatial variation of these properties is an excellent indicator of degradation. The *spectral profiling* made possible by the ESR imaging method, which was demonstrated in this study, is expected to be exceptionally sensitive to early events in the degradation process, and to be therefore of predictive value, and a dependable indicator of things to come.

Acknowledgment. This study was supported by the Polymers Program of the National Science Foundation. We thank J. L. Gerlock (Ford Research Laboratories) for his help in the preparation of the ABS plaques and for numerous illuminating discussions; M. Lucarini (University of Bologna, Italy) and A. Smirnov (University of Illinois at Urbana−Champagne) for their important help with the 1D simulation software; and Grzegorz Mazur (Jagiellonian University, Cracow, Poland) for his help with the 2D simulation software.

References and Notes

(1) Hill, D. J. T.; Le, T. T.; O'Donnell, J. H.; Perera, M. C. S.; Pomery, P. J. In *Irradiation of Polymeric Materials: Processes, Mechanisms, and Applications*; Reichmanis, E., Frank, C. W., O'Donnell, J. H., Eds.; American Chemical Society: Washington, DC, 1993.

(2) O'Donnell, J. H. In *The Effects of Radiation on High-Technology Polymers*; Reichmanis, E., O'Donnell, J. H., Eds.; American Chemical Society: Washington, DC, 1989; Chapter 1, p 1.

(3) Gerlock, J. L.; Bauer, D. R.; Briggs, L. M. *Polym. Degrad. Stab.* **1986**, *14*, Part I, p 53; Part II, p 73; Part III, p 97.

(4) Brede, O.; Beckert, D.; Windolph, C.; Gottinger, H. A. *J. Phys. Chem. A* **1998**, *102*, 1457. This paper provides a detailed summary of the current literature on the protective mechanism of HAS.

(5) Pospisil, J. *Adv. Polym. Sci.* **1995**, *124*, 87.

(6) *Polymer Durability: Degradation, Stabilization and Lifetime Prediction*; Clough, R.G., Billingham, N.C., Gillen, K. T., Eds.; Adv. Chem. Series 249, American Chemical Society: Washington, DC, 1996.

(7) McKenzie, R.; Connor, B.; Bodeker, G. *Science* **1999**, *285*, 1709.

(8) Schlick, S.; Pilar, J.; Kweon, S.-C.; Vacik, J.; Gao, Z.; Labsky, J. *Macromolecules* **1995**, *28*, 5780. Gao, Z.; Pilar, J.; Schlick, S. ESR *J. Phys. Chem.* **1996**, *100*, 8430. Kruczala, K.; Gao, Z.; Schlick, S. *J. Phys. Chem.* **1996**, *100*, 11427. Gao, Z.; Schlick, S. *J. Chem. Soc. Faraday Trans.* **1996**,

92, 4239. Malka, K.; Schlick, S. *Macromolecules* **1997**, *30*, 456. Schlick, S.; Eagle, P.; Kruczala, K.; Pilar, J. In *Spatially Resolved Magnetic Resonance: Methods, Materials, Medicine, Biology, Rheology, Ecology, Hardware;* Blümler, P., Blümich, B., Botto, R., Fukushima, E., Eds.; Wiley-VCH: Weinheim, 1998; Chapter 17, p 221. These papers describe the use of 2D spatial-spectral ESRI for measuring the diffusion coefficients of paramagnetic tracers.

(9) Degtyarev, E. N.; Schlick, S. *Langmuir* **1999**, *15*, 5040. This study has demonstrated the application of 1D ESRI for measuring the diffusion coefficients of tracers in self-assembled polymeric surfactants.

(10) Motyakin, V. M.; Gerlock, J. L.; Schlick, S. *Macromolecules* **1999**, *32*, 5463.

(11) *EPR Imaging and in Vivo EPR;* Eaton, G. R., Eaton, S. S., Ohno, K., Eds.; CRC Press: Boca Raton, FL, 1991. Figures 2 (p 138) and 5 (p 142) show the 2D spatial-spectral images of "phantoms" composed of two specimens, to illustrate the potential of the method.

(12) Ohno, K. In *EPR Imaging and in Vivo EPR*; Eaton, G. R., Eaton, S. S., Ohno, K., Eds.; CRC Press: Boca Raton, FL, 1991; Chapter 18, p 181. Figure 4 on p 186 presents a series of four 2D spatial-spectral ESR images of radicals in polypropylene containing Tinuvin after electron-beam irradiation. The images show the evolution of the line shapes, from polymer radicals to HAS-derived nitroxides, as a function of time. These temporal changes can also be observed by ESR spectroscopy.

(13) Lucarini, M.; Pedulli, G. F.; Borzatta, V.; Lelli, N. *Polym. Degrad. Stab.* **1996**, *53*, 9.

(14) Kweon, S.-C. M.Sc. *Thesis*. University of Detroit Mercy, 1993.

(15) Carter, R. O., III; McCallum, J. B. *Polym. Degrad. Stab.* **1994**, *45*, 1.

(16) Gillen, K. T.; Clough, R. L. *Polymer* **1992**, *33*, 4359.

(17) Gillen, K. T.; Clough, R. L.; Dhooge, N. J. *Polymer* **1986**, *27*, 225.

(18) Gillen, K. T.; Clough; R. L.; Quintana, C. A. *Polym. Degrad. Stab.* **1987**, *17*, 31.

(19) Gillen, K. T.; Clough, R. L.; Wise, J. In *Polymer Durability: Degradation, Stabilization and Lifetime Prediction*; Clough, R. G., Billingham, N. C., Gillen, K. T., Eds.; Adv. Chem. Series 249, American Chemical Society: Washington, DC, 1996; Chapter 34, p 557.